

THIS REPORT HAS BEEN DELIMITED
AND CLEARED FOR PUBLIC RELEASE
UNDER DOD DIRECTIVE 5200.20 AND
NO RESTRICTIONS ARE IMPOSED UPON
ITS USE AND DISCLOSURE.

DISTRIBUTION STATEMENT A

APPROVED FOR PUBLIC RELEASE;
DISTRIBUTION UNLIMITED.

Armed Services Technical Information Agency

Because of our limited supply, you are requested to return this copy WHEN IT HAS SERVED YOUR PURPOSE so that it may be made available to other requesters. Your cooperation will be appreciated.

AD

44978

NOTICE: WHEN GOVERNMENT OR OTHER DRAWINGS, SPECIFICATIONS OR OTHER DATA ARE USED FOR ANY PURPOSE OTHER THAN IN CONNECTION WITH A DEFINITELY RELATED GOVERNMENT PROCUREMENT OPERATION, THE U. S. GOVERNMENT THEREBY INCURS NO RESPONSIBILITY, NOR ANY OBLIGATION WHATSOEVER; AND THE FACT THAT THE GOVERNMENT MAY HAVE FORMULATED, FURNISHED, OR IN ANY WAY SUPPLIED THE SAID DRAWINGS, SPECIFICATIONS, OR OTHER DATA IS NOT TO BE REGARDED BY IMPLICATION OR OTHERWISE AS IN ANY MANNER LICENSING THE HOLDER OR ANY OTHER PERSON OR CORPORATION, OR CONVEYING ANY RIGHTS OR PERMISSION TO MANUFACTURE, USE OR SELL ANY PATENTED INVENTION THAT MAY IN ANY WAY BE RELATED THERETO.

Reproduced by
DOCUMENT SERVICE CENTER
KNOTT BUILDING, DAYTON, 2, OHIO

UNCLASSIFIED

81644
44978

WADC TECHNICAL REPORT 54-230

CREEP BEHAVIOR OF EXTRUDED ELECTROLYTIC MAGNESIUM

THE DOW CHEMICAL CO.

JUNE 1954

WRIGHT AIR DEVELOPMENT CENTER

BEST AVAILABLE COPY

WADC TECHNICAL REPORT 54-230

CREEP BEHAVIOR OF EXTRUDED ELECTROLYTIC MAGNESIUM

The Dow Chemical Company

June 1954

Aeronautical Research Laboratory
Contract No. AF 33(038) - 16655
RDO No. 463-6

Wright Air Development Center
Air Research and Development Command
United States Air Force
Wright-Patterson Air Force Base, Ohio

FOREWORD

This report was prepared by the Dow Chemical Company under Supplemental Agreement No. S2 (52-286) to USAF Contract Number AF 33(038)-36655. The contract was initiated under RDO 453-6, entitled "Principles of the Effect of Rare-Earth Additions on the High Temperature Properties of Magnesium". It was administered under the direction of the Aeronautical Research Laboratory (WCBRL), Directorate of Research, Wright Air Development Center, with Lt. John P. Hirth acting as project engineer.

ABSTRACT

The creep mechanism and kinetics of fine-grained magnesium have been studied over the temperature range 200 to 600F. As a result of a photographic study of microstructural changes, transient and steady-state creep components have been correlated with slip, subgrain formation, and cyclic deformation at the grain boundaries.

PUBLICATION REVIEW

This report has been reviewed and is approved.

FOR THE COMMANDER

Leslie B. Williams

LESLIE B. WILLIAMS

Colonel, USAF

Chief, Aeronautical Research Laboratory
Directorate of Research

TABLE OF CONTENTS

	<u>Page No.</u>
INTRODUCTION.	1
TENSILE CREEP VERSUS TIME, STRESS, AND TEMPERATURE. .	3
Transient Creep	5
Steady-State Creep.	5
DEFORMATION PROCESS IN CREEP.	6
Low-Temperature Type Deformation.	6
High-Temperature Type Deformation	7
DISCUSSION OF RESULTS	8
CONCLUSIONS	11
REFERENCES.	13

LIST OF ILLUSTRATIONS

<u>Figure</u> <u>Number</u>		<u>Page No.</u>
1	Preferred Orientation of Extruded Electrolytic Magnesium.	17
2	Creep Curves for Extruded Electrolytic Magnesium When Transient Creep is the Major Process.	18
3	Creep Curves for Extruded Electrolytic Magnesium When Steady-State Creep is the Major Process.	19
4	Semilog Plot of Stress Versus Secondary Creep Rate for Extruded Electrolytic Magnesium.	20
5	Log-Log Plot of Stress Versus Secondary Creep Rate for Extruded Electrolytic Magnesium.	21
6	Stress and Temperature Dependence of Transient Creep.	22
7	Plot for Determination of Temperature Coefficient Q_s of Transient Creep.	23
8	Electrolytic Magnesium After 0.04 Creep Strain at 200F and 6000 Psi. Stress Axis Vertical . .	24
9	Electrolytic Magnesium After 0.04 Creep Strain at 300F and 5500 Psi	24
10	Electrolytic Magnesium After 0.08 Creep Strain at 400F and 3675 Psi.	25
11a	Electrolytic Magnesium After 0.04 Creep Strain at 500F and 2000 Psi	26
11b	Electrolytic Magnesium After 0.04 Creep Strain at 500F and 2000 Psi	26
12	Electrolytic Magnesium After 0.041 Creep Strain at 600F and 1500 Psi.	27
13	Electrolytic Magnesium After 0.02 Creep Strain at 600F and 300 Psi.	27
14	Electrolytic Magnesium After 0.01 Creep Strain at 400F and 1000 Psi	28

LIST OF TABLES

Table
Number

Page No.

1	Stress and Temperature Dependence of $\beta, n,$ and m	16
---	---	----

CREEP BEHAVIOR OF EXTRUDED ELECTROLYTIC MAGNESIUM

INTRODUCTION

The approach of this research has been the blend of a quantitative study of the creep strain of polycrystalline magnesium as a function of time, stress, and temperature with direct microstructural observations of the operative deformation processes. The validity of the conclusions is dependent on the condition that the microstructural changes seen on the polished surface qualitatively represent those occurring in the bulk of the metal. The work was intended as much to lay a background to a study of highly creep-resistant magnesium alloys as to provide a description of the behavior of the base metal itself.

The spectroscopic analysis of the electrolytic magnesium used in this study is as follows: Al, 0.009%; Ca, <0.01; Cu, 0.0011; Fe, 0.021; Mn, 0.012; Ni, 0.0004; Pb, 0.0012; Si, <0.001; Sn, <0.001; and Zn, <0.01. The impurity level is approximately that of commercial magnesium alloys. The original ingot was melted under Dow type 310 flux and cast as a 3 inch diameter billet. It was extruded into 1-1/4 x 1/8 inch flat stock under the conditions: billet preheat 800F (1 hour), container and die temperature 800F, speed 3 feet per minute, and area reduction ratio 45:1. The extrusion process was chosen in preference to rolling and recrystallization because it allowed easier grain size control from specimen to specimen.

The grains of the extruded metal were fairly equiaxial and uniform in the size range of 4 to 6 thousandths of an inch. The preferred orientation of basal planes about the transverse direction was determined by an X-ray diffraction surface reflection method. A beam of filtered copper radiation was

directed at an angle of 17° to both the transverse direction and the surface yet perpendicular to the extrusion axis. Analysis of the (002) diffraction arcs in the resulting photographic patterns gave an approximate intensity distribution along the great circle which extends through the center of the basal plane pole figure and to the extrusion axis poles. Successive layers of metal were removed by macroetching between exposures.

The extruded texture is relatively sharp, but the most significant point is the position of the maximum basal plane pole density and its variation with depth below the surface. Figure 1 shows that this maximum is rotated 15° from the normal at the surface toward the extrusion direction. Such an inclination has been reported for extruded 1% Mn and 8% Al-0.5% Zn alloys⁽¹⁾. The inclination decreases until the maximum splits at about 0.025 inch depth into two elements of equal and opposite rotations from the ideal. The double texture persists to as great a depth as was experimentally convenient to examine. It probably continues to the very center of the extrusion. There is no great change in the sharpness of the individual elements of the texture with depth.

A plate of metal about 0.015 inch thick at the surface of the extruded stock was produced by etching. A transmission diffraction pattern was made for the purpose of determining any preferred orientation of a direction in the basal planes. Relatively uniform $\{100\}$ and $\{101\}$ rings were produced. There is little tendency for parallelism of a given direction in the plane with the projection of the extrusion axis on it.

The creep specimens were machined from 6-1/4 inch lengths of the extruded stock. Creep was measured on the reduced section, 1/2 x 1/8 x 2-1/4 inch long. This section was

electropolished on one side for the studies of microstructural changes during creep. An orthophosphoric acid-ethyl alcohol electrolyte was used under the conditions recommended by Jacquet(2). Hand polishing was used for previous mechanical preparation. Electropolishing was continued until all mechanical twins had been removed. The electropolished surface was protected from oxidation during creep testing by a thin layer of silicone oil. All micrographs were taken at room temperature on conventional metallographic equipment and after removal of the oil film.

The creep tests were performed with machines which have been described in detail by Moore and McDonald(3). Five testing temperatures, 200, 300, 400, 500, and $600 \pm 3^{\circ}\text{F}$ were used. Difference in temperature between the two ends of the specimen reduced section was 2°F or less. The testing was done at constant load. Strain readings were taken as frequently as necessary to develop usable creep curves.

TENSILE CREEP VERSUS TIME, STRESS, AND TEMPERATURE

A definition of terms is necessary. Whenever successive sections of a creep strain-time curve show decreasing, constant, and increasing slope with time they will be termed primary, secondary, and tertiary creep, respectively. The terms transient and steady-state creep will be applied in the conventional manner to the two separable elements which show finite decreasing and constant strain rates, respectively, from the beginning of the test. Primary creep may be used for a quantitative analysis of the transient component only when the steady-state creep is negligible. Secondary creep may be analyzed as steady-stage creep only when the transient element is negligible.

Quantitative analyses of the linear coordinate plots of creep strain versus time for magnesium proved the existence of both transient and steady-state components. Transient creep was predominant for all stresses tested at the lowest temperature of test, 200F. Steady-state creep becomes more predominant as the temperature increased and to a lesser extent as the stress decreased. There is negligible transient creep at the limit of low stresses at 600F. The representative creep curves shown in Figures 2 and 3 illustrate the change of curve shape over the experimental range of stress and temperature. Transient creep is predominant in the curves of Figure 2. Figure 3 illustrates the predominance of steady-state creep. Tertiary creep was never observed, although many tests were carried to a creep strain of 0.10.

In the first phase of this investigation creep curves were obtained from tests at the temperatures of 300, 400, 500, and 600F. Each test was continued until rectilinearity of the plot had demonstrated the existence of secondary creep. Secondary creep was never generated within the measurable strain range in the tests at 200F. The first kinetic analyses were made with secondary creep rate, stress, and temperature as the variables. Attempts were made to fit isothermal rate data to the exponential, power, and hyperbolic sine functions of stress. With the use of tables constructed for the purpose⁽⁴⁾ it was found that the latter function gave a poor fit of the data. Curvature of the semilog plot of stress versus secondary creep rate shown in Figure 4 constitutes proof of the invalidity of the exponential relation. The plot of the data on log-log coordinates in Figure 5 is a test of the power relation between stress and secondary creep rate. The rectilinearity of the isotherms proves the validity of the power function. A relatively sharp transition between two straight line segments

in each isotherm is required to fit the data. Such transitions have been reported and discussed by Servi and Grant (5) (6).

Transient Creep: The creep strain-time data for the higher stresses at 200, 300, 400, and 500F, where transient creep is very predominant, were plotted on log-log coordinates. Straight lines were obtained in agreement with the equation

$$\epsilon_t = \beta t^n$$

where ϵ_t is transient creep strain; β , a function of temperature and stress; t , the time in hours; and n , a constant.

Values of β and n , which are equal to the intercept at 1 hour and slopes of the straight line, respectively, are given in Table I. A remarkable constancy of n with an average value of 0.53 was found. The dependence of β on stress and temperature is shown in Figure 6. Straight and reasonably parallel lines prove that β is of the form $B(T)\sigma^m$ where m , the average slope in Figure 6, is 4.0. A straight line in the plot of β at 3000 psi versus the reciprocal of the absolute temperature, Figure 7, shows $B(T)$ to be of the form $Ae^{-Q/RT}$. The β values plotted are the intercepts of the lines in Figure 6, using extrapolation of the 500F data. The temperature coefficient Q , is equal to 15,500 cal per gram atom. In the experimental range, the average slope in Figure 6, is 4.0. Transient creep in the range of 200 to 500F and 1250 to 10,000 psi may be represented by:

$$\epsilon_t = 4.5 \times 10^{-9} e^{-\frac{15,500}{RT}} \sigma^{4.0} t^{0.53}$$

Steady-State Creep: Calculations were made of the transient creep rate $d\epsilon/dt$ which was occurring at the strain level of individual curves where the secondary creep rate was measured for the general kinetic analysis. Comparison of these rates

with the measured secondary rates led to an understanding of the transitions shown in Figure 5. The measured rates are predominantly the steady-state creep element on the high temperature-low stress side of a transition. Under conditions represented by the low temperature-high stress side of a transition, the measured rates are predominantly the transient creep element. Because of the markedly different stress dependence of the two rates, only in the near vicinity of a transition on the log-log plot are they of the same order of magnitude at the strain levels where the secondary rates were measured.

An analysis of the stress and temperature dependence of the steady-state creep element alone was made on the low stress segments of the isotherms of Figure 5. The only conclusion that could be drawn was that the steady-state creep coefficient, k , was a power function of stress with the exponent b a function of temperature. The separable element of temperature dependence showed no simple form. That is, steady-state creep in polycrystalline electrolytic magnesium may be represented by:

$$\epsilon_x = k (\sigma^{b(T)}, T)t.$$

DEFORMATION PROCESS IN CREEP

Low-Temperature Type Deformation: Several electropolished specimens were deformed at high creep rates. Figure 8 presents the microstructure of a specimen deformed at 200F. The microstructures shown in Figures 9 to 12 correspond to the test conditions labeled by the encircled numerals 1 to 4 in Figure 5. With the exception of the one produced at 400F, the structures may be directly compared at a total creep strain of about 0.04.

The slip lines are straight with a fineness and

uniformity of spacing which decrease with increasing temperature. The formation of sharp subgrains is common to all temperatures. The sharpness of the subboundaries is clearly shown with vertical illumination in Figure 10. At the lower strain level, oblique illumination is valuable in revealing their sharpness as in Figure 11b. In general, however, oblique illumination was avoided because of the excessive shadows produced at the grain boundaries. The slight deviation of slip lines which pass through the subboundaries and the results of a few X-ray back-reflection studies showed that neighboring subgrains were only slightly disoriented with respect to each other. In all of these structures deformation at the grain ~~boundaries is~~ much less than that within the grains. However, the boundary deformation increases in magnitude and changes from a rough and broken-up to a smooth appearance as the temperature increases.

High-Temperature Type Deformation: The smooth variety of grain boundary deformation is a cyclic process of sliding and migration which is best studied under conditions when it is predominant. Figures 13 to 14 which correspond to points 5 and 6 on the low-stress high-temperature segments in Figure 5 present microstructures obtained when primary creep was nearly absent. The mechanical twins and vertical polishing scratches which unfortunately appear in Figure 13 were present before testing because of insufficient electropolishing of this specimen only. All other specimens used in the research were free of twins and scratches after electropolishing. Subgrain formation has disappeared and slip lines are few in number. The ribbing of the displaced regions was the first clue to the cyclic nature of the process. Inspection of many grain boundaries revealed the following characteristics:

1. In almost all cases grain boundary sliding is such that the grain having the convex surface boundary contour subsides.

2. In all cases grain boundary migration is "downhill", i.e., into the subsided grain. Thus it is almost always in the normal direction for grain growth (grain boundary energy induced process).

Grain growth is negligible if specimens are annealed at temperatures and for times equal to those necessary to produce boundary migration in the cyclic deformation process. It is reasonable to regard the process as one of accelerated grain growth accompanied by the generation of strain. The process can lead to the ultimate consumption of grains as is shown in Figures 12 and 13. A series of photographs which also illustrates this point and which corresponds to point 7 in Figure 5 has been presented⁽⁷⁾.

DISCUSSION OF RESULTS

The cyclic grain boundary deformation process is perhaps the most striking one observed in this research. It has been observed and analyzed in the creep of polycrystalline aluminum by Servi and Grant⁽⁵⁾⁽⁶⁾ and Chang and Grant⁽⁸⁾⁽⁹⁾. The latter investigators employed precise measurements of creep across the boundaries to obtain cyclic creep curves which correlated with the alternate elements of sliding and migration. The structure resulting from this process appears in the micrographs of aluminum by Hanson and Wheeler,⁽¹⁰⁾ Wilms and Wood,⁽¹¹⁾ and McLean,⁽²⁹⁾ iron alloys by Jenkins and Mellor,⁽¹²⁾ zinc by Cottrell and Aytakin⁽¹³⁾ and Ramsey,⁽¹⁴⁾ tin-antimony alloy by Betteridge and Franklin,⁽¹⁵⁾ lead-thallium alloy by Gifkins,⁽¹⁶⁾ magnesium by Suiter and Wood,⁽¹⁷⁾ and tin by Puttick and King.⁽²⁷⁾

Sliding appears to occur in boundaries nearest to 45° to the stress axis until stopped by the local interference at

edges and vertices. The strain energy localized at the grain boundary regions then accelerates the activation of boundary migration. The migration evidently lowers the strain energy (local stress relief) and allows more sliding at the boundary. In other words, the process is guided by the tendency to lower both strain energy and surface energy. This was a conclusion reached in a previous study of aluminum.⁽⁹⁾ The sparseness of slip lines in Figures 13 and 14 indicates that in the limiting case of high temperature and low stress this process may be the sole mechanism of creep. The change of mass of the grain adds another degree of freedom not possessed by the deformation processes which lead only to change of grain shape.

The predominance of grain boundary deformation correlates with the predominance of steady-state creep. Perhaps the constancy of creep rate results from the existence of the cyclic self-recovery which boundary migration provides. The whole picture developed from these studies of creep rate and microstructural changes supports the concept of transient creep resulting from deformation within the grains and steady-state creep from grain boundary deformation. This viewpoint was first presented by Andrade⁽¹⁸⁾⁽¹⁹⁾ and has since been supported by many investigators⁽²⁰⁾⁽¹¹⁾⁽¹³⁾⁽¹⁵⁾⁽⁵⁾⁽⁶⁾.

Although transient creep in magnesium obeys the power function of time, the exponent, 0.53, differs from the classical value $1/3$. This is in contrast with the work on zinc by Cottrell and Aytakin⁽¹³⁾ and that on aluminum by Servi and Grant⁽⁵⁾ where agreement was found. This difference may be due to the testing conditions of constant load rather than constant stress. If this were the cause, it would hardly seem possible to obtain such consistent results,

however. The exponential relation between transient creep and temperature has been found to hold over a range of 300F (167C) for extruded electrolytic magnesium. It has been proven for nickel over a 75C range by Hazlett and Parker⁽²¹⁾ and for zinc, aluminum, and magnesium over a 100C range by Crussard.⁽²²⁾ The latter investigator reported Q for magnesium as ranging from 16,000 to 18,000 cal per gram atom, a good agreement with the result of this research. There is no evidence that Q can be identified as the activation energy of any simple rate-controlling process.

The occurrence of twinning was not found in any of the microstructural studies of extruded magnesium. This can be understood **after** an examination of the preferred orientation, Figure 1. When basal planes lie at small angles to the tension axis, twinning is not to be expected. However, recent work on very coarse grained magnesium by Chaudhuri et al.⁽²³⁾ and the studies of zinc by Cottrell and Aytakin⁽¹³⁾ and magnesium by Suiter and Wood⁽¹⁷⁾ have shown that when orientation conditions allow it twinning plays an important part in creep behavior. Recent work on the rare-earth alloys of magnesium in this laboratory has elucidated the roles of twinning and also of non-basal slip in creep deformation. The results will be reported elsewhere.

The significance of subgrain formation in the creep deformation of aluminum, zinc and magnesium has been well established.⁽⁶⁾⁽¹¹⁾⁽¹³⁻¹⁵⁾⁽¹⁷⁾⁽²³⁾⁽²⁴⁾⁽²⁸⁾ The similarity of this polycrystalline deformation process to kinking and polygonization phenomena in single crystals has been discussed by Washburn and Parker.⁽³⁰⁾ They illustrate how continuity at grain boundaries may be aided by the occurrence of subgrain formation. It has been concluded in some of the past investigations that the process is of importance only at high

temperatures and low creep rates and further that there is an appreciable increase of subgrain size with increasing temperature. The present results show that subgrain formation in magnesium is most pronounced at high creep rates at all temperatures. As the creep rate decreases at a given temperature, it disappears before slip does. The cyclic boundary deformation serves as its successor. The microstructural studies show no appreciable change in subgrain size over the entire experimental range of temperature and creep rate.

The results show that with increasing temperature and decreasing stress, predominance in creep changes from the processes of slip and subgrain formation to that of grain boundary deformation. It seems possible that at very low stresses and at temperatures approaching the melting point, the viscous self-diffusion process postulated by Nabarro⁽²⁵⁾ and Herring⁽²⁶⁾ may become predominant. All these processes must overlap each other in operation. Nevertheless, transitions may be expected from one to the other as the major creep rate-controlling process.

Fortunately it is becoming more and more apparent as time passes that there is more similarity than difference in the creep mechanism and kinetics of polycrystalline metals. The agreement between studies of magnesium, aluminum, and zinc points out that although minor differences may be of technical importance, they can generally be integrated into a coherent picture of the fundamentals.

CONCLUSIONS

1. The creep strain of extruded polycrystalline electrolytic magnesium over the temperature range 200 to 600F consists of both transient and steady-state elements. The two elements

of creep strain may be represented as a function of time, stress and temperature by:

$$\epsilon = 4.5 \times 10^{-9} e^{-\frac{15,500}{RT}} \sigma^{4.0} t^{0.53} + k(\sigma^b(T), T)t.$$

2. A rather sharp transition occurs between two straight line segments of the isotherms in the log-log plot of stress versus observed secondary creep rate. This results from the markedly different stress and temperature dependence of the two creep components.

3. The transient component of creep results from the intragranular processes of basal slip and subgrain formation. It is of major importance at low temperatures and/or high stresses.

4. The steady-state element of creep results from a cyclic process of sliding and migration of the grain boundaries. It is predominant at high temperatures and/or low stresses.

5. Slip lines become coarser and less uniformly spaced as the creep temperature increases.

6. The size of subgrains formed in creep is independent of creep rate and temperature over the experimental range studied.

REFERENCES

1. R. L. Dietrich, "Surface Orientation and Rolling of Magnesium Sheet." Trans. AIME (1949) 185, page 621; Journal of Metals (September 1949).
2. P. A. Jacquet, "Electrolytic Polishing of Metallic Surfaces and Its Applications (1948) page 64. Saint-Germain-En-Laye. Editions Metaux.
3. A. A. Moore and J. C. McDonald, "Tensile and Creep Strengths of Some Magnesium-Base Alloys at Elevated Temperature". Proc. ASTM (1946) 46, page 970.
4. P. G. McVetty, "Creep of Metals at Elevated Temperatures. The Hyperbolic-Sine Relation Between Stress and Creep Rate". Trans. ASME (1943) 65, page 761.
5. I. S. Servi and N. J. Grant, "Creep and Stress Rupture Behavior of Aluminum As a Function of Purity". Trans. AIME (1951) 191, page 909; Journal of Metals (October 1951).
6. I. S. Servi and N. J. Grant, "Structure Observations of Aluminum Deformed in Creep at Elevated Temperatures. Trans. AIME (1951) 191, page 917; Journal of Metals (October 1951).
7. C. S. Roberts, Discussion on Ref. 8; Trans. AIME (1953) 197, page 732; Journal of Metals (May 1953).
8. H. C. Chang and N. J. Grant, "Observations of Creep of the Grain Boundary in High Purity Aluminum". Trans AIME 1952 194, page 619; Journal of Metals (June 1952).
9. H. C. Chang and N. J. Grant, "Grain Boundary Sliding and Migration and Intercrystalline Failure Under Creep Conditions." Trans. AIME (1953) 197, page 305; Journal of Metals (February 1953).
10. D. Hanson and M. A. Wheeler, "The Deformation of Metals Under Prolonged Loading. Part I--The Flow and Fracture of Aluminum." Journal Inst. Metals (1931) 45, page 229.

11. G. R. Wilms and W. A. Wood, "Mechanism of Creep in Metals". Journal Inst. Metals (1949) 75, page 693.
12. C. H. M. Jenkins and G. A. Mellor, "Investigation of the Behavior of Metals Under Deformation at High Temperatures. Part I--Structural Changes in Mild Steel and Commercial Irons During Creep." Journal Iron and Steel Inst. (1935) 132, page 179.
13. A. H. Cottrell and V. Aytakin, "The Flow of Zinc Under Constant Stress". Journal Inst. Metals (1950) 77, page 389.
14. J. A. Ramsey, "Some Observations on the Deformation of Polycrystalline Zinc." Journal Inst. Metals (1951) 80, page 167.
15. W. Betteridge and A. W. Franklin, "An Investigation of the Structural Changes Accompanying Creep in a Tin-Antimony Alloy". Journal Inst. Metals (1951) 80, page 147.
16. R. C. Gifkins, "Grain Movements During Creep." Nature (1952) 169, page 238.
17. J. W. Suiter and W. A. Wood, "Deformation of Magnesium at Various Rates and Temperatures". Journal Inst. Metals (1952) 81, page 181.
18. E. N. daC. Andrade, "On the Viscous Flow in Metals, and Allied Phenomena". Proc. Royal Soc. (1911) 84, page 1.
19. E. N. daC. Andrade, "The Flow in Metals Under Large Constant Stresses". Proc. Royal Soc. (1914) 90, page 329.
20. E. Orowan, "Creep of Metals". Journal West Scotland Iron and Steel Inst. (1947) 54, page 45.
21. T. H. Hazlett and E. R. Parker, "Nature of the Creep Curve". Trans. AIME (1953) 197, page 318; Journal of Metals February 1953).

22. C. Crussard, "The Role of Grain Boundaries in the Deformation of Metals. Application to Creep and Fatigue". Revue Metallurgie (1946) 43, page 307.
23. A. R. Chaudhuri, N. J. Grant, and J. T. Norton, "Metallographic Observations of the Deformation of High-Purity Magnesium in Creep at 500F". Trans. AIME (1953) 197, page 712; Journal of Metals (May 1953).
24. J. A. Ramsey, "The Subgrain Structure in Aluminum Deformed at Elevated Temperatures". Journal Inst. Metals (1952) 81, page 215.
25. F. R. N. Nabarro, Report of Conference on the Strength of Solids (1948) page 75. London. Physical Society.
26. C. Herring, "Diffusional Viscosity of a Polycrystalline Solid". Journal of Applied Physics (1950) 21, page 437.
27. K. E. Puttick and R. King, "Boundary Slip in Bicrystals of Tin". Journal Inst. Metals (1951-1952) 80, page 537.
28. D. McLean, "Crystal Fragmentation in Aluminum During Creep." Journal Inst. Metals (1952-1953) 81, page 227.
29. D. McLean, "Grain-Boundary Slip During Creep of Aluminum". Journal Inst. Metals (1952-1953) 81, page 293.
30. J. Washburn and E. R. Parker, "Kinking in Zinc Single-Crystal Tension Specimens". Trans. AIME (1952) page 1076; Journal of Metals (October 1952).

TABLE 1
Stress and Temperature Dependence of β , n , and m

Temperature F	Stress Psi	n	β	m
200	3,000	0.58	0.00019	
	4,500	0.58	0.00088	
	6,000	0.56	0.0034	
	8,000	0.50	0.0124	
	10,000	0.53	0.0285	
	Average	0.55		4.2
300	2,500	0.49	0.0018	
	3,500	0.50	0.0066	
	4,000	0.50	0.0110	
	5,000	0.54	0.0260	
	6,000	0.55	0.0450	
	Average	0.53		3.9
400	1,200	0.53	0.00048	
	1,500	0.49	0.00145	
	1,750	0.49	0.00265	
	2,000	0.51	0.0055	
	2,500	0.51	0.0113	
	3,000	0.49	0.0220	
	3,500	0.53	0.0500	
	Average	0.51		4.2
500	1,250	0.54	0.0082	
	1,750	0.54	0.0285	
	2,250	0.53	0.0580	
	Average	0.54		3.5
Average		0.53		4.0

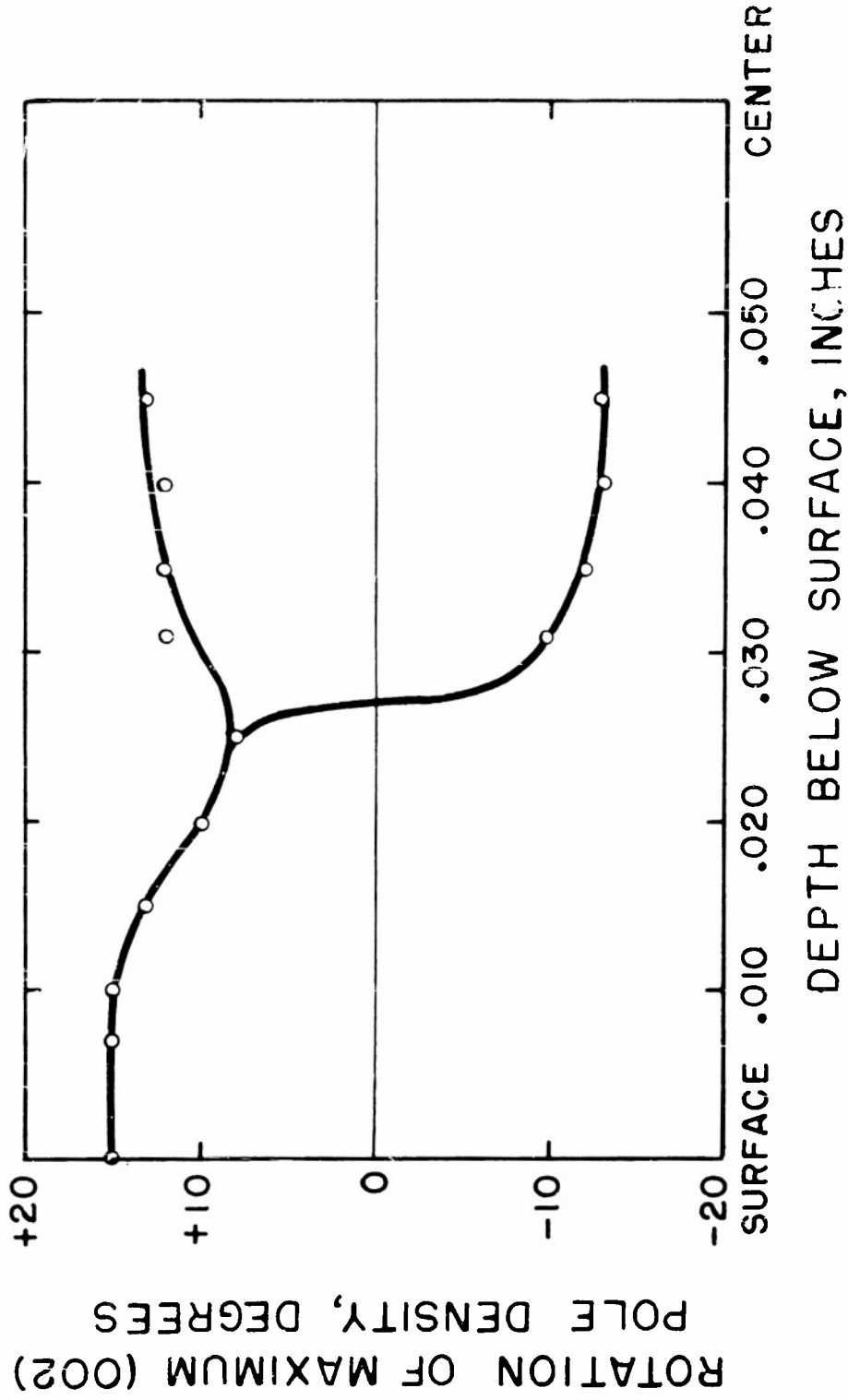


Fig. 1. Preferred Orientation of Extruded Electrolytic Magnesium. Positive Angles Toward Extrusion Direction.

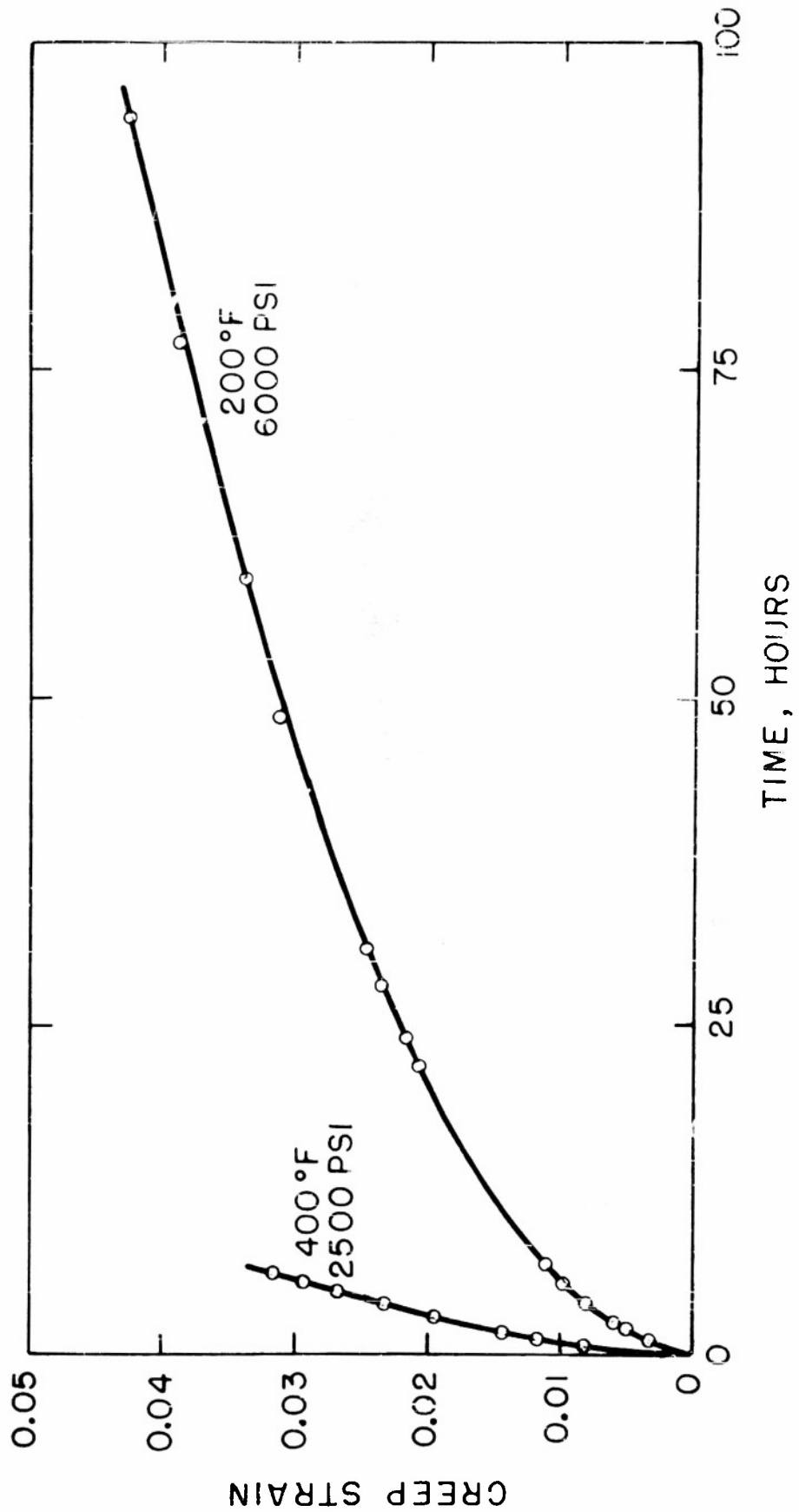


Fig. 2. Creep Curves for Extruded Electrolytic Magnesium when Transient Creep is the Major Process

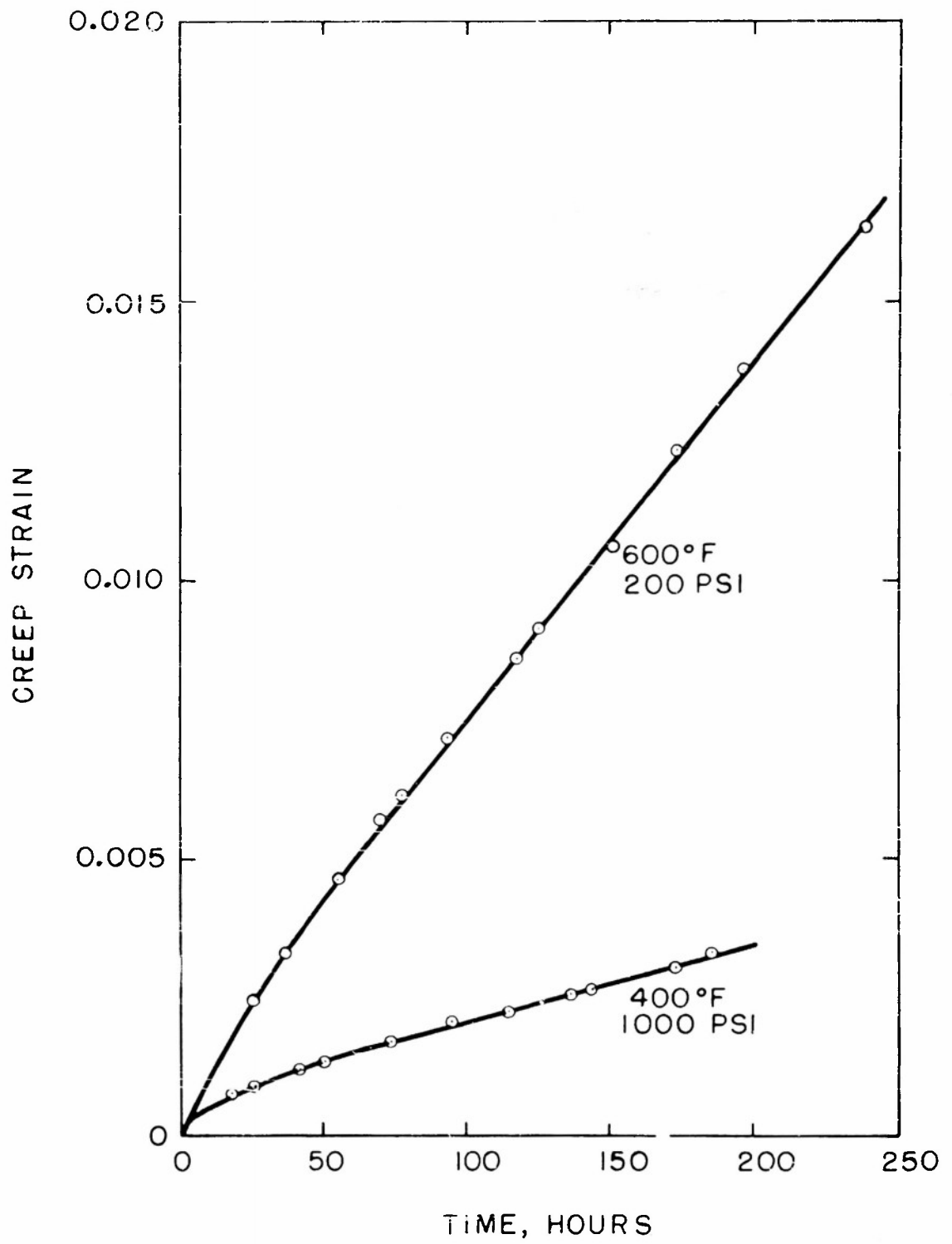


Fig. 3. Creep Curves for Extruded Electrolytic Magnesium When Steady-State Creep is the Major Process.

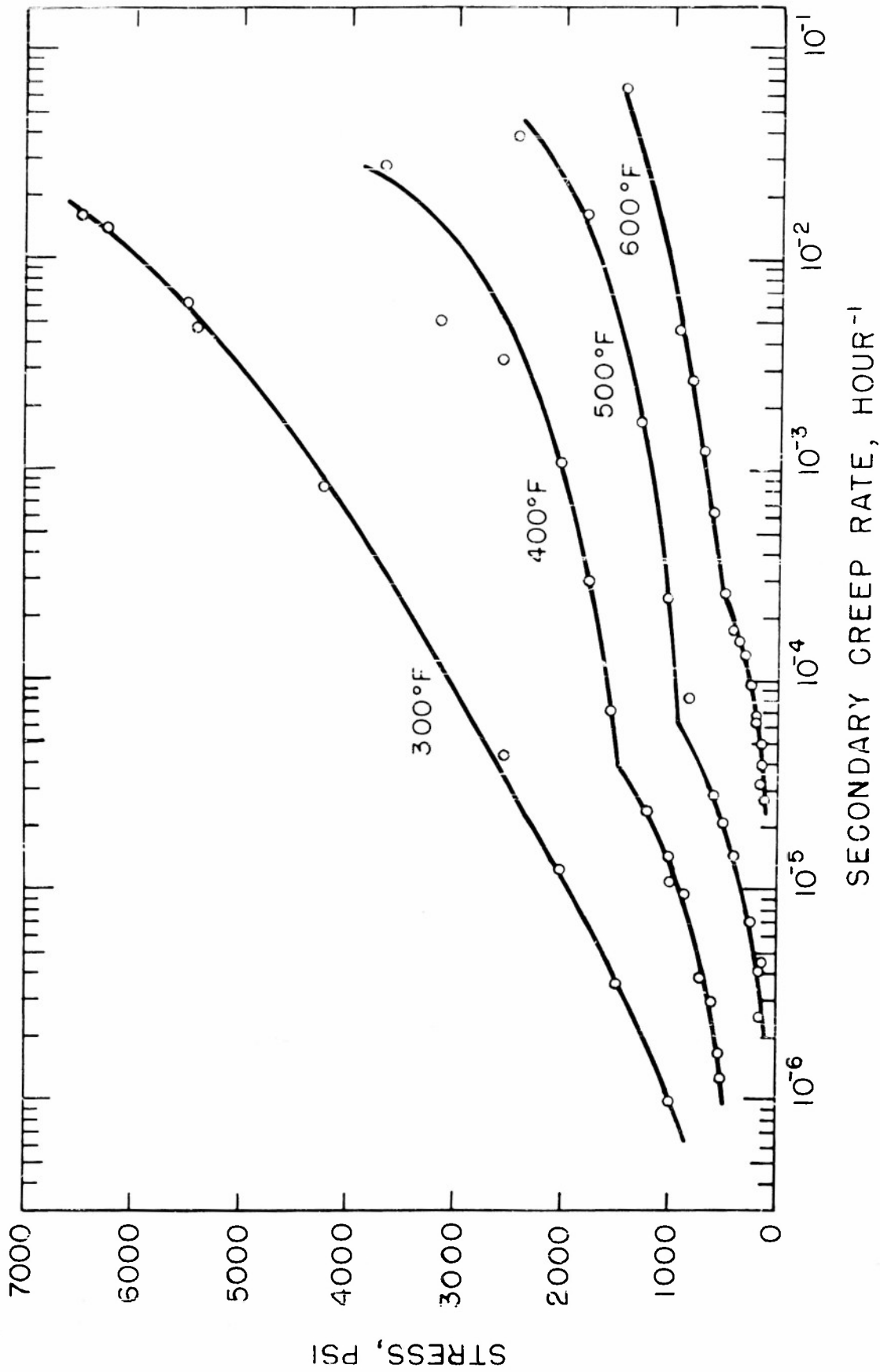


Fig. 4. Semi-log Plot of Stress vs Secondary Creep Rate for Extruded Electrolytic Magnesium.

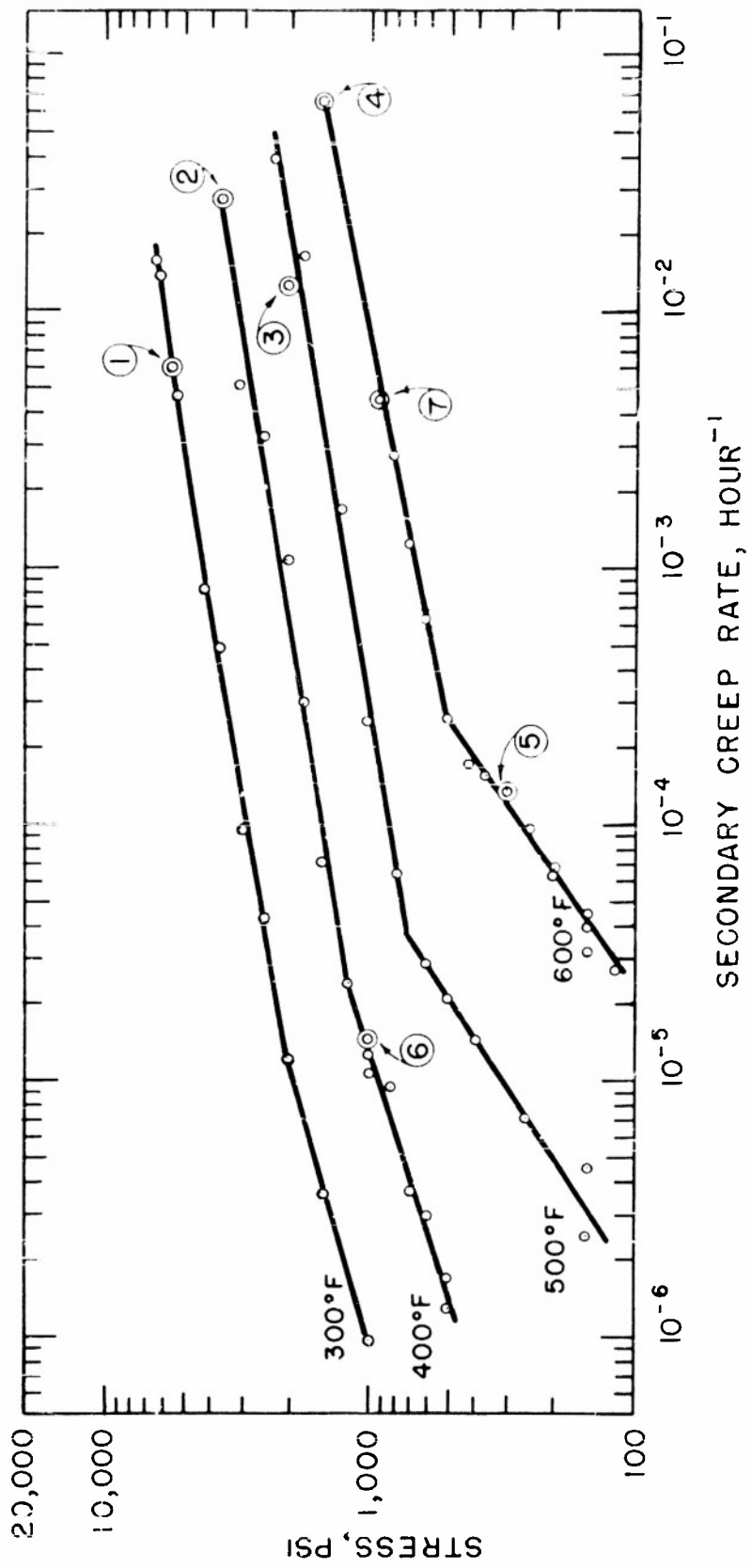


Fig. 5. Log-log Plot of Stress vs Secondary Creep Rate for Extruded Electrolytic Magnesium.

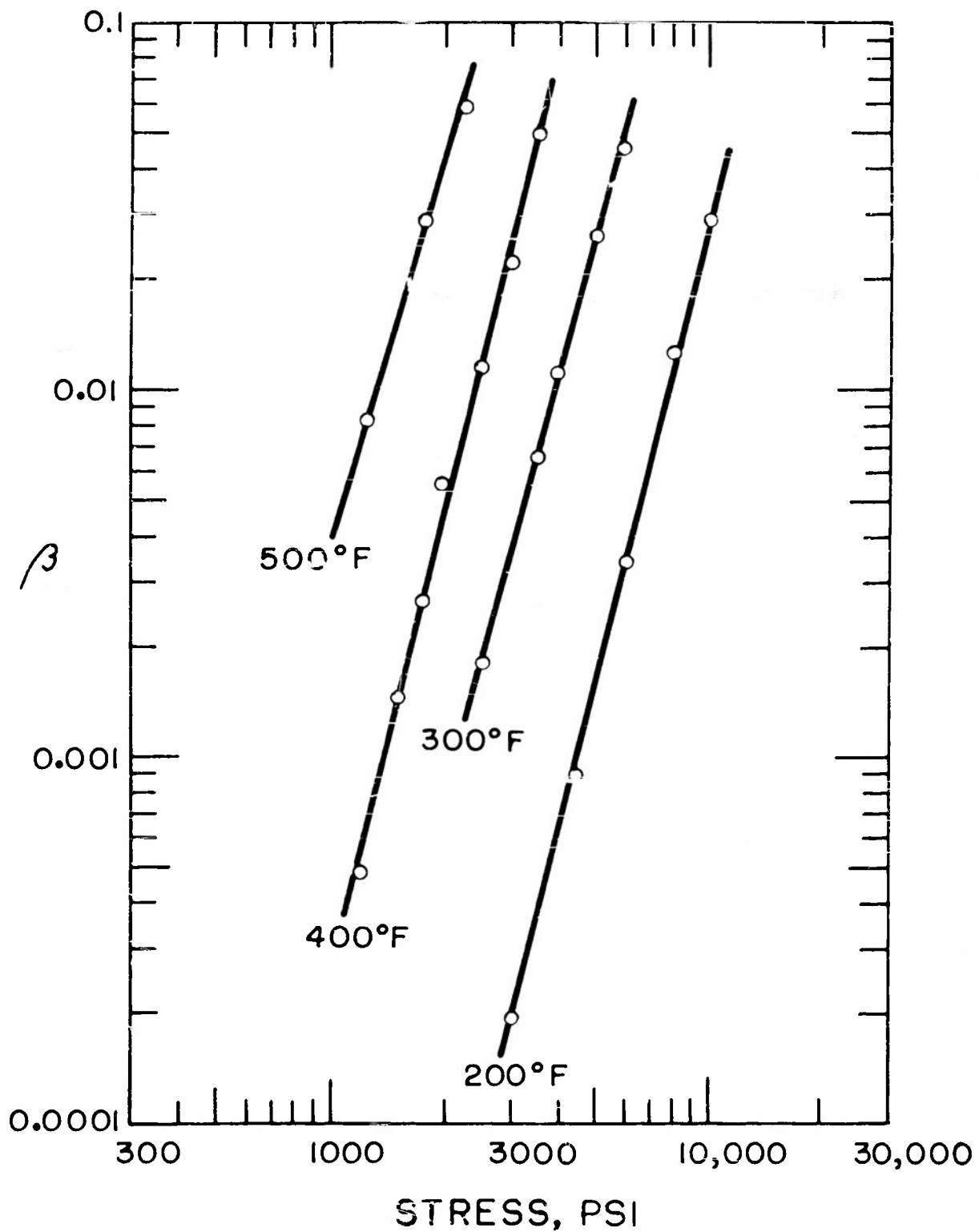
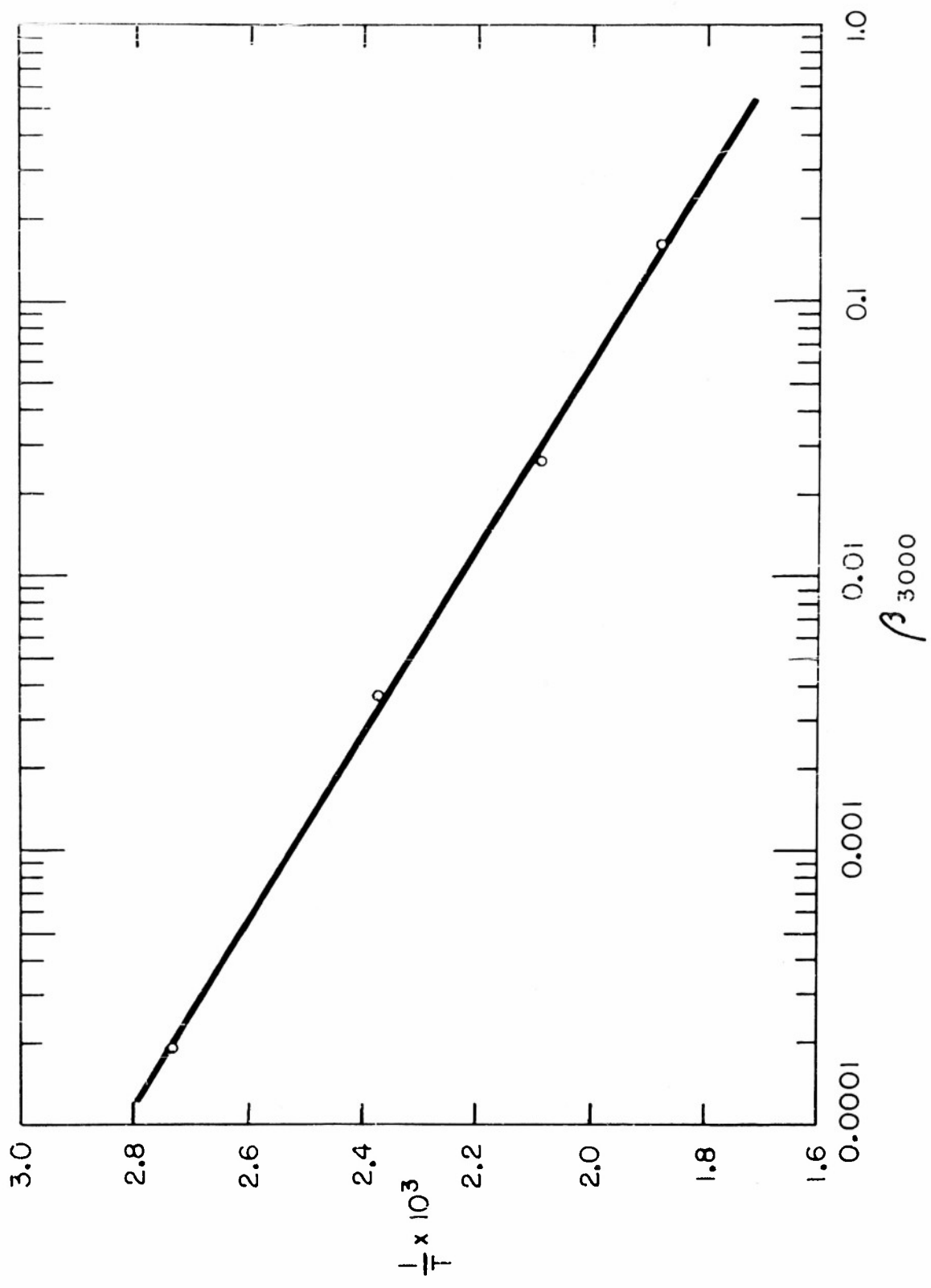


Fig. 6. Stress and Temperature Dependence of Transient Creep.



WADC TR 54-230

Fig. 7 Plot for Determination of Temperature Coefficient Q, of Transient Creep.



FIGURE 8 250X
Electrolytic Magnesium After 0.04 Creep
Strain at 200F and 6000 Psi. Stress Axis
Vertical.



FIGURE 9 250X
Electrolytic Magnesium After 0.04 Creep
Strain at 300F and 5500 Psi, Conditions
of Point 1 in Figure 5. Stress Axis
Vertical.



FIGURE 10 250X
Electrolytic Magnesium After 0.03 Creep
Strain at 400F and 3675 Psi, Conditions
of Point 2 in Figure 5. Stress Axis
Vertical.



FIGURE 11a 250X
Electrolytic Magnesium After 0.04 Creep Strain at 500F and 2000 Psi, Conditions of Point 3 in Figure 5. Stress Axis Vertical. Vertical Illumination.



FIGURE 11b 250X
Electrolytic Magnesium After 0.04 Creep Strain at 500F and 2000 Psi, Conditions of Point 3 in Figure 5. Stress Axis Vertical. Oblique Illumination.



FIGURE 12 250X
Electrolytic Magnesium After 0.041 Creep
Strain at 600F and 1500 Psi, Conditions
of Point 4 in Figure 5. Stress Axis
Vertical.



FIGURE 13 250X
Electrolytic Magnesium After 0.02 Creep
Strain at 600F and 300 Psi, Conditions of
Point 5 in Figure 5. Stress Axis Vertical.



FIGURE 14 250X
Electrolytic Magnesium After 0.01 Creep
Strain at 400F and 1000 Psi, Conditions
of Point 6 in Figure 5. Stress Axis
Vertical.

Armed Services Technical Information Agency

Because of our limited supply, you are requested to return this copy WHEN IT HAS SERVED YOUR PURPOSE so that it may be made available to other requesters. Your cooperation will be appreciated.

AD

44978

NOTICE: WHEN GOVERNMENT OR OTHER DRAWINGS, SPECIFICATIONS OR OTHER DATA ARE USED FOR ANY PURPOSE OTHER THAN IN CONNECTION WITH A DEFENSE RELATED GOVERNMENT PROCUREMENT OPERATION, THE U. S. GOVERNMENT THEREBY INCURS NO RESPONSIBILITY, NOR ANY OBLIGATION WHATSOEVER; AND THE FACT THAT THE GOVERNMENT MAY HAVE FORMULATED, FURNISHED, OR IN ANY WAY SUPPLIED THE SAID DRAWINGS, SPECIFICATIONS, OR OTHER DATA IS NOT TO BE REGARDED BY IMPLICATION OR OTHERWISE AS IN ANY MANNER LICENSING THE HOLDER OR ANY OTHER PERSON OR CORPORATION, OR CONVEYING ANY RIGHTS OR PERMISSION TO MANUFACTURE, USE OR SELL ANY PATENTED INVENTION THAT MAY IN ANY WAY BE RELATED THERECO.

Reproduced by
DOCUMENT SERVICE CENTER
KNOTT BUILDING, DAYTON, 2, OHIO

UNCLASSIFIED